Investigation of the structural order in amorphous GeTe-based alloys

E. Carria[1], A. Mio[2], G. D'Arrigo[3], C. Bongiorno[3], C. Spinella[3], R. De Bastiani[1], M.G. Grimaldi[1] and E. Rimini[2]

[1]*Dipartimento di Fisica ed Astronomia, Università di Catania and MATIS CNR-INFM, 64 via S. Sofia, I-95123 Catania, Italy*
[2] *Dipartimento di Fisica ed Astronomia, Università di Catania and CNR-IMM, 64 via S. Sofia, I-95123 Catania, Italy*
[3]*CNR-IMM, Stradale Primosole, 50, 95121 Catania, Italy*

Abstract

The crystallization kinetics of as-deposited (sputtered), laser quenched and ion implanted amorphous $Ge_2Sb_2Te_5$ (GST) and GeTe thin films have been measured by time resolved reflectivity. An enhancement of the crystallization process occurred in the ion and laser irradiated samples. Raman scattering analysis and transmission electron microscopy measurements were used to correlate the stability of the amorphous phase to its structure. Ion implantation tends to modify the atomic arrangement of the amorphous phase and facilitate the transition to the octahedral crystalline state. The local rearrangement of the amorphous network is suggested to be related to thermal spikes effects rather than to the defects produced by the ions in the collision cascade.

Introduction

The amorphous to crystal transition and the stability of the amorphous phase are of practical interest in the GeTe-based alloys for their use in optical storage and recently in non-volatile memories. The working principle is based on the substantial difference of optical and electrical properties of the amorphous and crystalline phase respectively [1]. The change reflects the different bonding arrangements between the two phases from tetrahedral to octahedral coordination and vice-versa [2]. This behaviour is quite unusual if one considers monatomic semiconductors, as Si or Ge.

In the last years, extensive experimental studies have focussed on the amorphous to crystal phase transformation. It has been reported that different amorphous states exist for the Ge-Sb-Te system, with a crystallization kinetics depending on their structure [3-6]. Crystallization of a melt-quenched amorphous is an order of magnitude faster than that of sputter-deposited amorphous GST [3]; moreover the crystallization velocity of the deposited amorphous has been reported to depend on the sample thermal history. All of these evidences pointed out the necessity of a close inspection of the structure of amorphous state prepared in different ways, and their influence on the crystallization kinetics.

In this study, the details controlling the phase stability of as-deposited (sputtered), laser quenched and ion irradiated amorphous $Ge_2Sb_2Te_5$ and GeTe chalcogenide thin films have been investigated by means of *in situ* time resolved reflectivity measurements, transmission electron

microscopy, *ex situ* Raman scattering spectroscopy and Radial Distribution Function obtained by electronic diffraction. The as-deposited amorphous layers were irradiated at room or liquid nitrogen temperature by Sb^+ or Ge^+ ions at different energies and at a fluence of $1x10^{14}$ ions/cm^2. An enhancement of the crystallization kinetics occurred in laser and ion irradiated amorphous samples compared to the as-deposited films for both alloys. Raman scattering spectroscopy and electron diffraction analyses were used to correlate the stability of the amorphous phase to its structure and clarify the nature of the different phase transition process.

Experimental

$Ge_2Sb_2Te_5$ and GeTe amorphous films, 40 nm thick, were prepared by rf sputter deposition at room temperature (R.T.), from a stoichiometric target, over oxidized Si wafers. As-deposited amorphous samples were irradiated at R.T. with 130 keV Ge^+ or 120 keV Sb^+ ions at fluence of $1x10^{14}$ ions/cm^2. Some samples were implanted at the liquid nitrogen temperature (LN_2) to ascertain the recombination effect of the defects induced by ion irradiation. The ions projected range, by SRIM (Ref. 7) calculations, was ~ 54 nm (ΔR_P ~ 24 nm) and ~ 40 nm (ΔR_P ~ 20 nm) respectively. The beam current was kept constant to 100 nA to avoid heating of the sample. The dose and the beam energy were chosen in such a way to avoid any appreciable change in the stoichiometry of the sample and to provide a nearly uniform energy loss in nuclear encounters, across the sample. Other chalcogenides samples were at first crystallized and subsequently irradiated with high power Nd:YAG 10 ns pulse laser to melt the layer. The high quenching rate induces the formation of an amorphous layer.

The crystallization of unirradiated and laser or ion irradiated amorphous films was followed by *in situ* time resolved reflectivity (TRR) using a low power He–Ne laser probe during annealing in the range 120 - 165 °C. The heating rate was 10 °C/min and the settled temperature was constant within ± 0.1 °C. The reflectivity increase has been converted into the crystalline fraction, f_S, by using the effective medium approximation [8].

Room temperature unpolarized micro-Raman spectra were recorded in a backscattering geometry using a single spectrometer. The chalcogenides samples were excited with a He-Ne laser (λ=633 nm). The laser power was adjusted to 6 mW in order to avoid heating effects in the illuminated sample region.

The morphology of the partially crystallized samples were investigated by TEM and atomic force microscopy (AFM) analyses. Transmission electron microscopy, in plan view configuration, was performed using a JEOL JEM 2010F TEM/STEM equipped with a 200-kV Schottky field-emission electron gun, and an ultra high-resolution objective lens pole piece.

Discussion

Figure 1(a-b) shows the crystallized fraction obtained by reflectivity signal during the annealing, for as-deposited unirradiated (open circles) and irradiated (open triangles) amorphous $Ge_2Sb_2Te_5$ and GeTe films respectively. The zero of the time scale is the time at which the settled temperature is reached. In the unirradiated sample the reflectivity remains initially constant. After

this transient it increases abruptly and saturates at the crystalline value when the crystallization is complete and the polycrystalline phase is formed.

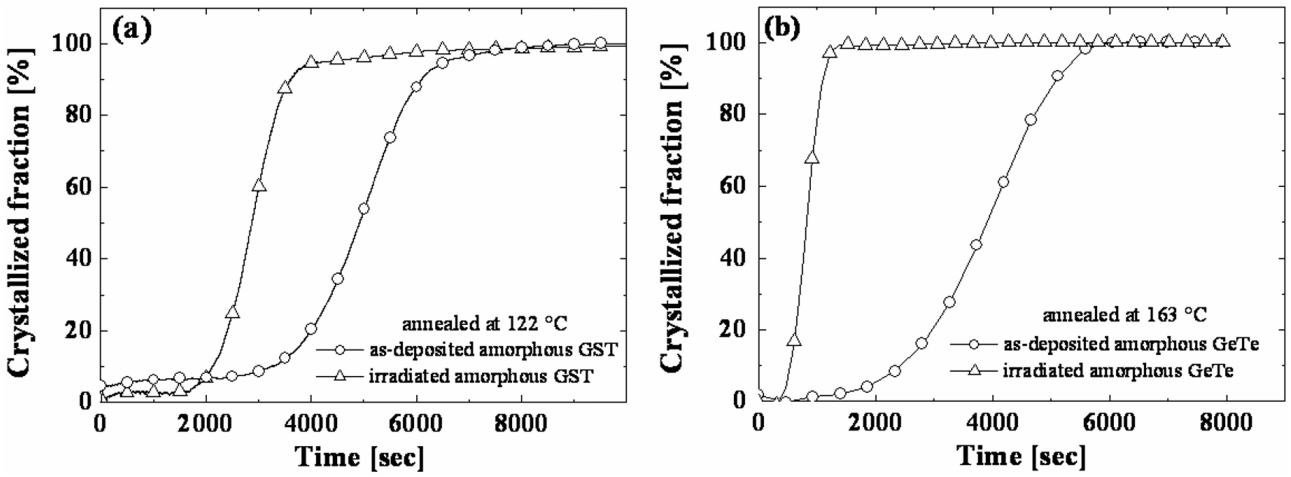

Figure 1 (a) Crystallized fraction, obtained by reflectivity vs annealing time at 122 °C for as-deposited amorphous $Ge_2Sb_2Te_5$ (open circles) and Sb^+ irradiated amorphous films at a fluence of $1x10^{14}$ at./cm^2 (open triangles) performed at room temperature. **(b)** Crystallized fraction, obtained by reflectivity vs annealing time at 163 °C for as-deposited amorphous GeTe (open circles) and Ge^+ irradiated amorphous films at a fluence of $1x10^{14}$ at./cm^2 (open triangles) performed at room temperature.

A similar trend occurs in the irradiated samples although the time evolution of the reflectivity signal indicates that the crystallization process is faster in the implanted amorphous layer with respect to the unirradiated amorphous film. Amorphous samples irradiated at the same fluence at the liquid nitrogen temperature (not reported) show an identical transition curve into the polycrystalline phase. This unambiguously demonstrates that any dynamic annealing process occurring during the implantation does not change the density of the defects responsible for the crystallization enhancement and that the main effect of irradiation is associated to the prompt regime of the collision cascade and not to the delayed effect, influenced by the movement of the displaced atoms.

The amorphous sample obtained by laser irradiation shows a much faster crystallization compared to the as-deposited and ion irradiated samples. The faster crystallization of melt-quenched amorphous layer has been attributed to the presence of small cluster of atoms similar to that of crystalline phase that reduce drastically the incubation time. It has been reported that these embryos are the nuclei of the hexagonal phase and that the grain growth is caused by these nuclei [9]. Moreover, there is no evidence of transrotational [10] structures during the transition to the crystal phase; this behaviour should be linked to a different density between as-deposited and laser irradiated amorphous samples.

To obtain a direct, although qualitative, influence of the different initial amorphous structures on the subsequent crystallization, GST and GeTe samples were analyzed by *in situ* heating in a transmission electron microscope. To directly compare unirradiated and irradiated amorphous, some samples were prepared implanting Sb^+ or Ge^+ ions at a fluence of 10^{14} ions/cm^2 through a mask

consisting of a copper grid, with holes and bar width of 36 μm and 25 μm respectively, placed at the sample surface. In this way selectively implanted regions next to unimplanted areas were formed. Fig. 2(a) shows a bright-field TEM image of the film surface after 15 min anneal at 130 °C.

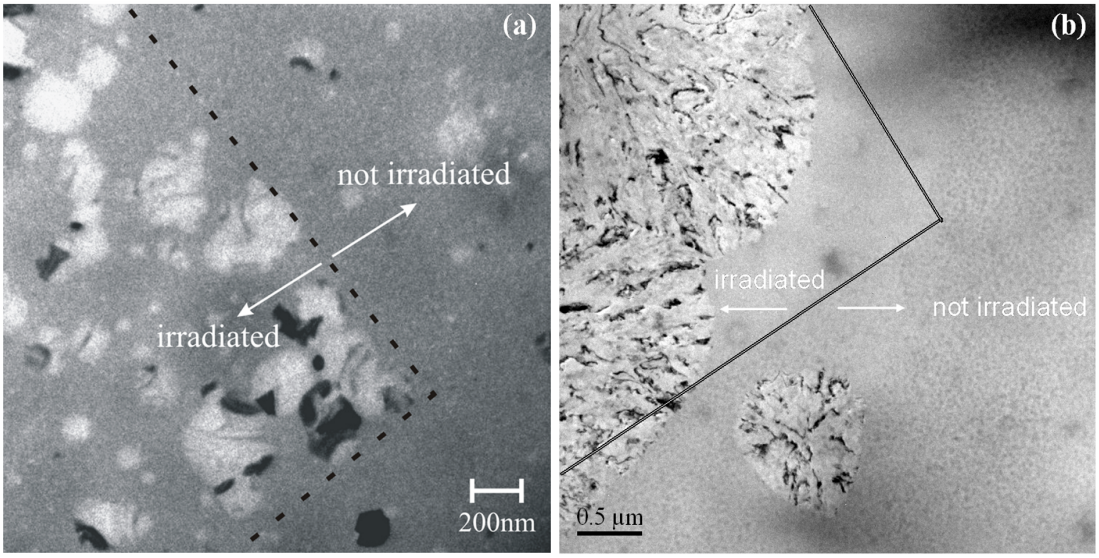

Figure 2 (a) TEM plan-view micrographs of partially crystallized as-deposited amorphous $Ge_2Sb_2Te_5$ and GeTe **(b)** films implanted with Sb^+ or Ge^+ ions respectively; the presence, during implantation, of a copper mask placed on the sample surface has produced selectively implanted areas next to not implanted areas. On the implanted region the grains have very large fringes and uniform contrast. Outside this region the grains show narrow fringes with a dark spot at the center of each transrotational crystal grain.

At this temperature, crystallization occurs inside and outside the ion irradiated area. However a different morphology (of grains) in the implanted and unimplanted regions is clearly visible. In the unirradiated area the grains exhibit the typical contrast of transrotational structures characterized by dark fringes corresponding to bending contours which move laterally by tilting the sample around axes parallel to the fringes themselves [11-12]. Another peculiarity is the presence of bright and dark small spots (20 nm of diameter), localized at the center of each transrotational crystal grain or just surrounded by amorphous regions. No dimpled crystalline are detected in the implanted region. In this region the grains show very large fringes and a quite uniform contrast. This means that the degree of internal bending decreases. Moreover, in this last zone the density of crystalline nuclei is higher than that in unirradiated region. In other words, ion irradiation strongly influences the morphology and the crystallization kinetics of the phase transition. Similar results were obtained for crystalline GeTe films implanted with 130 keV Ge^+ ions as shown in figure 2b where is reported a bright-field TEM image of the film surface after 15 min anneal at 165 °C.

The occurrence of the transrotational structures has been related to the difference between the atomic density of the crystal and the amorphous phase. Indeed, because of the elastic deformation due to the density change, as these crystallites grow a bending of the lattice plane at the lateral a-c interface occurs to minimize the elastic energy due to the strain. To check if the bending reduction in the irradiated samples derives from a density variation because of the ion-solid interaction we

analyzed, by means of atomic force microscopy, the morphology of the irradiated and unirradiated regions, previously described, of an amorphous layer. The AFM analysis of the irradiated region, (not shown), indicates that the ion beam induces a reduction of the film thickness observed as a depression, with respect the surface of the unirradiated regions. This reduction is comparable to that observed at the boundaries of crystalline domains in unirradiated samples, due to the density change upon crystallization. The density increase reduces the elastic energy associated to the strain of the phase transition and a structure with a lower internal bending is formed.

The short-range order of several $Ge_2Sb_2Te_5$ and GeTe amorphous states, has been investigated using Raman spectroscopy. Figure 3 (a) shows the Raman spectra of as-deposited, irradiated amorphous films at a fluence of $1x10^{14}$ Sb/cm^2 and laser-amorphized crystalline film with an energy density of 80 mJ/cm^2. Two well separated bands appear in the frequency range of 100–250 cm^{-1} of the deposited amorphous GST film (open circles); approximate wavenumber positions of these bands are 129 cm^{-1} and 152 cm^{-1}. The peak at 129 cm^{-1} has been attributed to vibrational bands of GeTe tetrahedra according to Ref. 5. The local structure of laser-amorphized crystalline GST (open triangles) is similar to that of as-deposited amorphous film as shown by the similarity in the Raman spectra, unlike ion implanted amorphous films (open squares) that exhibit remarkable changes in the relative intensity of the two peaks. In fact, the fraction of the tetrahedral species that constitute the glass structure, decreases after irradiation and the vibrational band at ~ 150 cm^{-1} becomes the only mode clearly distinguishable.

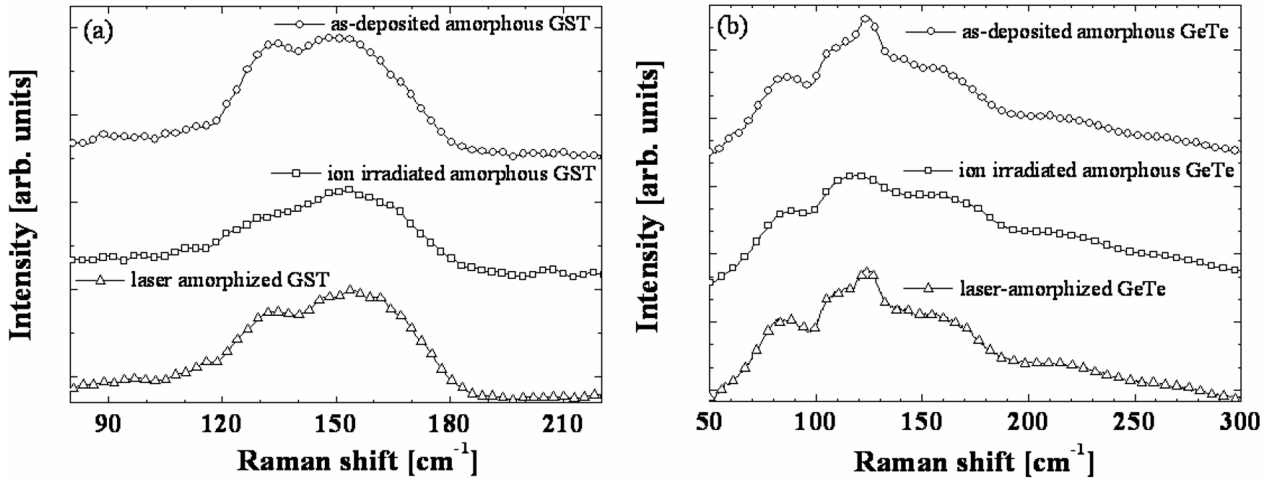

Figure 3 (a) Raman spectra of as-deposited amorphous $Ge_2Sb_2Te_5$ films (open circles), implanted with 120 keV $1x10^{14}$ Sb/cm^2 (open squares) and laser irradiated crystalline film (open triangles) with an energy density of 80 mJ/cm^2. **(b)** Raman spectra of as-deposited amorphous GeTe films (open circles), implanted with 130 keV $1x10^{14}$ Ge/cm^2 (open squares) and laser irradiated crystalline film (open triangles) with an energy density of 90 mJ/cm^2.

During the ion beam irradiation one might assume that Ge-Te tetrahedral bonds, characteristics of the Ge coordination in amorphous GST, can be selectively broken as observed also during the crystallization process [2]. The reduction of these bonds enhances the atomic diffusivity and

consequently the crystallization process as by TRR measurements. This trend confirms that the stability of the amorphous phase is controlled mainly by the covalent Ge-Te bonds.

The Raman spectrum of the as-deposited amorphous GeTe is reported in Fig. 3(b) (open circles). Six main contributions, with various intensities, are clearly visible in this spectrum. Approximate wavenumber positions of these bands are: ~ 86 cm^{-1}, 110 cm^{-1}, 125 cm^{-1}, 156 cm^{-1}, 211 cm^{-1} and 270 cm^{-1}. Amorphous layers obtained by laser quenching show the same local order as observed in the as-deposited sample. The spectrum of the irradiated amorphous GeTe shows remarkable changes in the relative intensity of the strongest Raman bands ascribed to the $GeTe_{4-n}Ge_n$ tetrahedral units. In particular a decrease of the lighter Ge-rich tetrahedral species could be the cause of the reduction of the band at 125 cm^{-1}. As a consequence, the amorphous stability decreases, as detected by *in situ* TRR measurements. A similar effect was observed at the beginning of the crystallization process of unirradiated amorphous GeTe samples. The local rearrangements obtained after irradiation, promotes the system to a state closer to the crystalline structure. This intermediate state, prior to the crystallization process, is probably achieved by ion-induced thermal spike effects.

In dense collision cascade at the end of the displacements spike, the energy is dissipated as lattice vibration or heat. The duration of the thermal spike can be estimated as $t \sim r^2/4D_T$, where r is the dimension of the collision cascade and D_T the thermal diffusivity of the target (~$3x10^{-2}$ cm^2/sec) (ref. 13). Assuming as an order of magnitude a radius r of about 10 nm, characteristic of the collision cascade lateral extension at the adopted projectile mass and energy and target composition, the quenching time or duration of the thermal spike amounts to ~10^{-11} sec. The typical crystallization times in several chalcogenides (GST, GeTe) run from hours at low temperatures (~ 150 °C) to few hundredth nanoseconds at temperatures below the melting point. The process is thermally activated with an energy of about 2 eV. These values imply a huge pre-exponential factor [14] in all the rate (nucleation rate, crystal growth), orders of magnitude higher than that observed in semiconductors. The same factor might be invoked to justify the ion-induced effect here reported. For diffusion limited crystallization, the grain growth velocity u is related to the atomic diffusivity D in the amorphous by $u = f_S \cdot 6D/\lambda$, where λ is the average interatomic distance and f_s<1 is the fraction of sites where a new atom can be incorporated. Assuming that a local bond rearrangement, requires a diffusivity of 0.5 nm during the life-time of the thermal spike, a temperature of ~ 870 K is needed. The melting point of GeTe or GST is well above the previous estimate. Although the previous discussion is based on order of magnitude, it seems plausible to justify the influence of the ion beam causing the selective bonds rearrangement.

Electronic scattering cross section allowed the analysis of amorphous diffraction patterns. The reduced radial distribution functions shown in Fig. 4 refer to as-deposited (full lines) or ion irradiated (dashed lines) GST [Fig. 4(a)] or GeTe [Fig. 4(b)] films, respectively. We note that ion irradiation produces a slight broadening of the distribution peaks mainly in the GST sample. This is probably related to the ion induced disorder. At these stages this kind of analysis does not allows us to get more detailed information on the difference in the local bonding arrangement of the two amorphous phases (as-deposited or after irradiation).

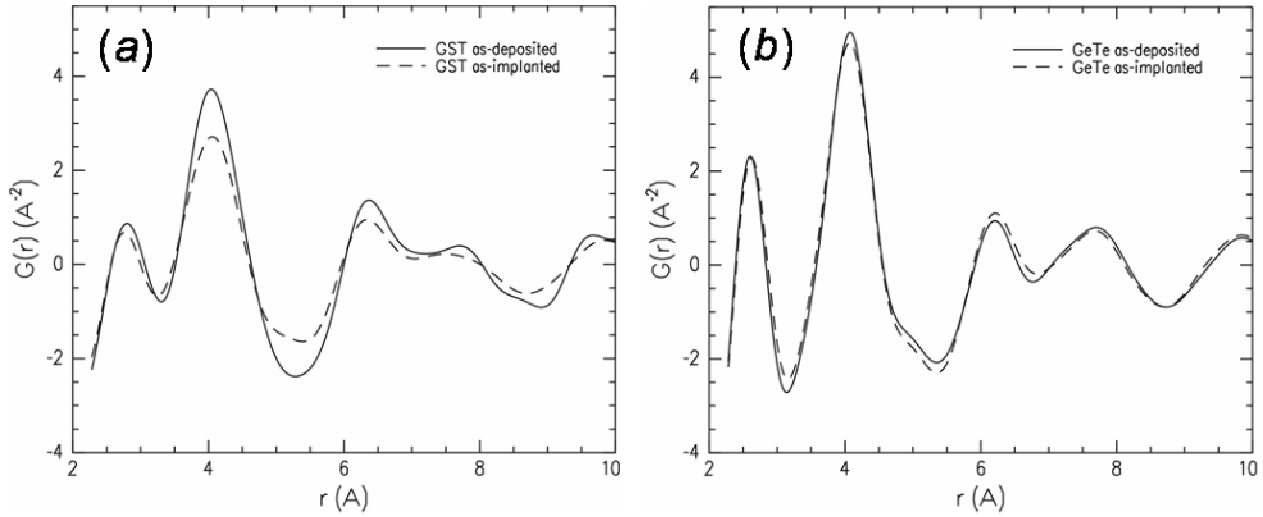

Figure 4(a) Reduced radial distribution function of as-deposited amorphous (full line) and implanted GST film with 100 keV 1×10^{14} Sb/cm^2 (dashed line). **(b)** Reduced radial distribution function of GeTe as-deposited amorphous (full line) and implanted with 130 keV 1×10^{14} Ge/cm^2 (dashed line).

Conclusion

In conclusion, we have analyzed by Raman spectroscopy different amorphous chalcogenides thin films: as deposited, laser and ion irradiated $Ge_2Sb_2Te_5$ and GeTe thin films. The local structure of laser-amorphized chalcogenide films was found similar to that of as-deposited amorphous samples for both alloys. Implanted samples exhibit remarkable alterations of the local order. A correlation between the amorphous phase stability and the percentage of Ge-Te bonds in the $Ge_2Sb_2Te_5$ and GeTe films has been presented. These local bonding rearrangements, associated to thermal spike effects of the collision cascade, cause an enhancement in the crystallization kinetics and a different grain morphology.

References

[1] A. Pirovano, A. L. Lacaita, A. Benvenuti, F. Pellizzer, S. Hudgens, and R. Bez, Tech. Dig. - Int. Electron Devices Meet. **2003**, 699.

[2] A. V. Kolobov, P. Fons, A. I. Frenkel, A. L. Ankudinov, J. Tominaga, and T. Uruga, Nat. Mater. **3**, 703 (2004).

[3] V. Weidenhof, I. Friedrich, S. Ziegler and M. Wuttig J. Appl. Phys. **89** (2001).

[4] P. Khulbe, E. Wright, M. Mansuripur, J. Appl. Phys. **88**, 3926 (2000).

[5] R. De Bastiani, A. M. Piro, M. G. Grimaldi, E. Rimini, G. A. Baratta, and G. Strazzulla, Appl. Phys. Lett. **92**, 241925 (2008).

[6] E. Rimini, R. De Bastiani, E. Carria, M. G. Grimaldi, G. Nicotra, C. Bongiorno, and C. Spinella, J. Appl. Phys. **105**, 123502 (2009).

[7] J. F. Ziegler, J. P. Biresack, and U. Littmark, *The Stopping and the Range of Ions in Solids* (Pergamon, New York, 1985).

[8] D. Kim, F. Merget, M. Laurenzis, P. H. Bolivar, and H. Kurz, J. Appl. Phys. **97**, 083538 (2005).

[9] M. Youm Y. Kim, M. Sung, Appl. Phys. Let. **91**, 083508 (2007).
[10] B. J. Kooi and J. Th. M. De Hosson, J. Appl. Phys. **95**, 4714 (2004).
[11] A. Alberti, C. Bongiorno, B. Cafra, G. Mannino, E. Rimini, T. Metzger, C. Mocuta, T. Kammler, and T. Feudel, Acta Crystallogr., Sect. B: Struct. Sci. **B61**, 486 (2005).
[12] V. Yu Kolosov, A. R. Tholén Acta Mater. **48**, 1829 (2000).
[13] J. M. Yáñez-Limón, J. González-Hernández, J. J. Alvarado-Gil, I. Delgadillo, and H. Vargas, Phys. Rev. B 52, 16321 (1995).
[14] S. Privitera, S. Lombardo, C. Bongiorno, E. Rimini, and A. Pirovano, J. Appl. Phys. **102**, 013516 (2007).

Biographies

Emanuele Rimini

Full Professor of Structure of Matter from 1976, – University of Catania. Director of the Institute for the Microelectronics and Microsystems (IMM-CNR) 2002-2008. **Fellow** of the American Physical Society- Division of Materials Science -1994 "For his pioneering contributions to the fields of particle-solid and laser-solid interactions and his leadership in establishing research consortia."

The research activity has spanned the following areas: point and extended defects in metals, channeling and de-channeling of light ions, analysis of defects and of impurity lattice location, thin film reaction, ion implantation, laser annealing, melting and solidification at extremely conditions, ion beam mixing, silicide formation, ion beam assisted regrowth, mesoscopic effects in low – dimensional materials science, silicide phase transition (C49-C54 TiSi2) in narrow strips, non volatile memories based on silicon nanocrystals embedded in silicon dioxide, morphology and structure of nanocrystals, analysis of the amorphous to polycrystal transition in chalcogenide material, fabrication and electrical characterization of single-photon optical detectors. He has published more than 350 articles , 15 chapters in books and edited 6 books. He has chaired several international conferences on ion implantation and ion beam modification.